Assessment of the New Superconducting Rock Magnetometer (SRM) on The *JOIDES Resolution*

SRM Team:
Gary Acton[1], Antony Morris[2], Robert Musgrave[3], and Xixi Zhao[4]

IODP SRM Personnel[5]: Brad Clement, Helen Evans, Margaret Hastedt, David Houpt, Bill Mills, Beth Novak, and Katerina Petronotis

[1]Department of Geography and Geology, Sam Houston State University, Huntsville, Texas, 77341-2148, USA. E-mail: gdacton@shsu.edu.
[2]School of Geography, Earth and Environmental Sciences, University of Plymouth, Plymouth PL4 8AA, UK. E-mail: amorris@plymouth.ac.uk
[3]Geological Survey of New South Wales, 516 High Street, Maitland, NSW 2320, Australia. E-mail: robert.musgrave@industry.nsw.gov.au
[4]State Key Laboratory of Marine Geology, Tongji University, Shanghai 200092, China. E-mail: xzhao@tongji.edu.cn.
[5]International Ocean Discovery Program, Texas A&M University, 1000 Discovery Drive, College Station, TX 77845-9547, USA.

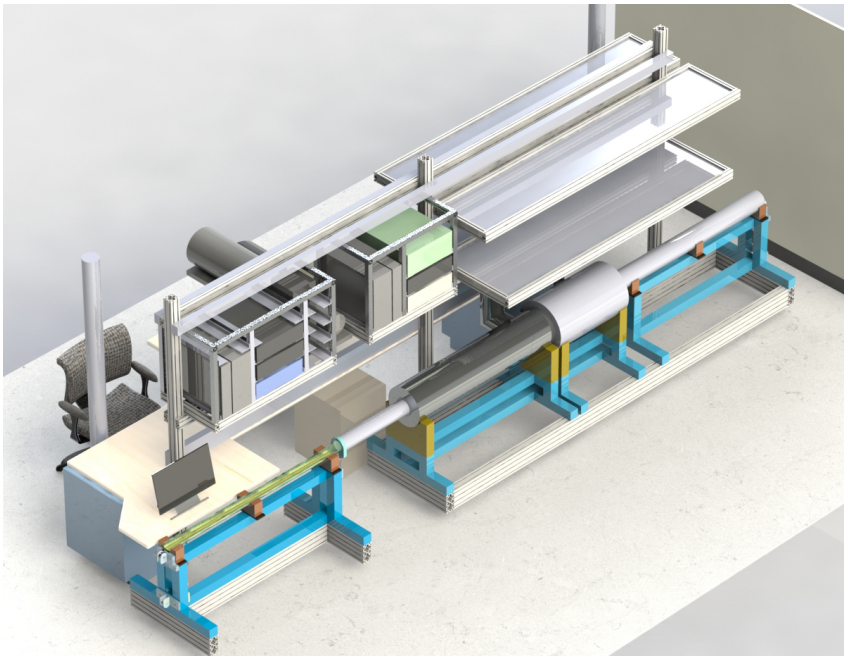

Shanghai, China, Port Call
11-13 June 2017

Table of Contents

Acronyms for instrument models and software

SRM: Superconducting Rock Magnetometer
New SRM: 2G Enterprises Model 760R-4K, no. 152 (the 50th liquid helium free system)
Old SRM: 2G Enterprises Model 760R, no. 60
JR-6A: The AGICO spinner magnetometer, Model JR-6A
IMS: Integrated Measurement System (version IMS 9.2), which is the new SRM software.

Introduction

The SRM Team was assembled to assess the new superconducting rock magnetometer (SRM) (Figure 1). This instrument had only been on the *JOIDES Resolution* (*JR*) for Expeditions 366, 367, and 368. Development of a new software package for operating and interrogating the SRM, called the Integrated Measurement System (IMS), began on Expedition 362, where testing was done with the old SRM, and has continued with the new SRM by the Shipboard Paleomagnetists on the past three expeditions.

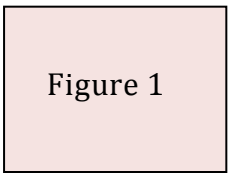

Figure 1. A photograph of the new SRM with a whole-round core section that was measured as part of the tests.

The SRM Team consisted of four paleomagnetists (Gary Acton, Tony Morris, Bob Musgrave, and Xixi Zhao) and the IODP staff with expertise in paleomagnetism (Brad Clement, Helen Evans, Maggie Hastedt, David Houpt, Bill Mills, Beth Novak, and Katerina Petronotis). All the team except for Evans convened at the Shanghai port call at the end of Expedition 368. The short port call (June 11-13, 2017) provided the SRM Team a fairly brief opportunity to run a series of tests and to make recommendations for future tests and improvements.

Our primary conclusion is that the new magnetometer is functioning as designed and performed better than (or at least comparable to) the previous magnetometer. Data to support this conclusion are provided below, as well as additional data and information on the function of the new SRM.

Initial Error Reports

As part of the assessment, we began by reviewing comments from the shipboard paleomagnetists who had used the new SRM on the previous three expeditions. Testing during the latter two of those cruises had suggested that the magnetometer had given suspicious results. Part of the error reports pertained to measurements made on very weakly magnetized sediments. It was unclear if the problems were related to the noise level of the magnetometer relative to the weak magnetizations or if other more significant issues existed. Specific issues raised in feedback from these expeditions and during a brief meeting between the Expedition 368 and SRM teams onboard the *JR* included:

- "*Measurement of sections proved difficult in the case of weakly magnetic sediments and due to a significant drilling overprint in materials with soft magnetic assemblages. The 3-D position of the split core on the track does*

seem to affect reproducibility and accuracy. Issues regarding zeroing of drift and background between sections were rectified by Bill Mills."

- *"Measurement of discrete samples shows that the magnetization intensities differ by over an order of magnitude between discrete samples and sections (both measured on the SRM)."*
- *"Differences larger than one order of magnitude were also observed between discrete samples measured both on the SRM and JR-6A. This suggests that the SRM may not be properly calibrated and that the current SQUIDS might be too sensitive to precise position of the specimen*."
- It was also reported that discrepancies in directions and intensities between JR-6A and SRM results were not systematic, suggesting the apparent difference in response between the two instruments may not simply be a matter of calibration. To illustrate the problem, the Expedition 368 paleomagnetists provided the SRM Team with a data file of results from four discrete samples measured on the JR-6A and data from corresponding archive half section intervals measured on the new SRM, both for multiple demagnetization steps between 0 and 20 mT.
- Discrepancies in SRM measurement were inferred to relate to the radial position of the sample within the coils: This effect supposedly depended on whether the sample was at the periphery or near the center of the sensor coils. It was suggested that there was a problem with where the sample sits within the sensor coils.

SRM Calibration Constants

We first assessed the calibration of the new SRM. The vendor (2G Enterprises) provides the calibration constants for the SRM based on a common standard used for all their magnetometers. Hence, the calibration should be consistent with other 2G Enterprises magnetometers. Those values (representing the coil response in emu/volt) are listed in the software and in all the SRM output files uploaded into the LIMS Database. They are:

$$X = 8.1036 \times 10^{-5}$$
$$Y = -8.2590 \times 10^{-5}$$
$$Z = 3.8825 \times 10^{-5}$$

The negative sign for the Y-axis SQUID presumably relates to converting the SQUID XYZ coordinate system from the left-handed system defined by 2G Enterprises to a right-handed system, which is then used in subsequent IODP computations.

Orientation within the new software (IMS) is accomplished by rotating the measured X, Y, and Z magnetic moments into the appropriate sample coordinates, depending on how the sample is collected and whether it is from the working or archive half. The IODP coordinate system is described and illustrated in IODP Technical Note 34 (Richter et al., 2007).

The calibration constants had been re-checked by Bill Goodman from 2G Enterprises at the port call in Hong Kong at the beginning of Expedition 368. He confirmed they were correct and provided a calibration coil for IODP, which now resides in the shipboard lab (Figure 2). This calibration coil was designed to give values within about 3% of those obtained with the primary 2G Enterprises calibration coil. The primary coil calibration constants are still used by IODP. The new calibration coil is merely used to check that the current calibration constants are consistent with those initially provided.

Given the recent calibration check by 2G Enterprises, we conducted only a few additional tests of the SRM calibration: 1) We measured the JR-6A calibration standards in the SRM discrete tray, providing a direct comparison to the JR-6A calibration; 2) we compared results of measurements of discrete samples made on the JR-6A and the new SRM; and 3) we measured igneous and sedimentary core sections on the new SRM, which had previously been measured on the old SRM. These tests are discussed in detail below. Overall, the results are generally comparable, with the new and old SRM results agreeing very well (see the "Comparison of the New SRM to the Previous SRM" section below). The new SRM, however, gave moments for the JR-6A calibration standards slightly (about 5%) lower than the JR-6A (see the "Response Function" section below). We did not have time to investigate if this difference was statistically significant and, if so, which instrument might need adjusting. We recommend that additional tests be conducted by shipboard paleomagnetists, who might bring along stable samples that have been accurately measured in their own labs before coming to the ship. This would allow comparison with the shipboard magnetometers and provide valuable inter-lab comparisons for the paleomagnetism community.

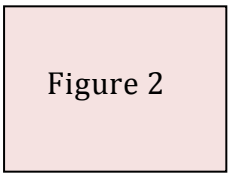

Figure 2. A calibration coil used for the SRM.

Response Functions

For discrete samples, the magnetization intensities are computed by dividing the X, Y, and Z magnetic moments by the volume of each sample. This simple approach does not work for long samples (samples longer than about 5 to 10 cm) because the X, Y, and Z sensor coils each senses over a different length and hence each senses a different volume of the sample. Moreover, the response of each of the sensor coils is not a constant ("boxcar") function over a certain length, but rather varies as a symmetric wavelet function (shaped somewhat like a "bell curve" or the cross-section of a "Sombrero"). To account for this

behavior, an effective length L_i is calculated from the response function for each of the three axes to represent the boxcar response, which would be equivalent to the integrated contribution of the actual response.

As discussed in IODP Technical Note 34 (Richter et al., 2007), the response functions are multiplied by the cross-sectional area of long samples to give the effective volume (V_e) measured by each axis of the magnetometer. The volume is used to compute the intensities as described in the following excerpt from the technical note.

The effective volume (V_e) and intensities for each sensor are determined as follows:

$V_{ex} = L_x A$

$V_{ey} = L_y A$

$V_{ez} = L_z A$

where A is the cross sectional area of a long sample

$A = 0.5\pi r^2$ *for split cores with a radius of r and*

$A = \pi r^2$ *for whole cores*

ODP core liners have an internal radius of approximately 3.3 cm.

The magnetization per unit volume J is obtained by normalizing the magnetic moments by the effective volume:

$J_x = M_x/V_{ex}$

$J_y = M_y/V_{ey}$

$J_z = M_z/V_{ez}$

The response functions were not initially provided by the vendor but can be computed by measuring a point dipole source as it is moved through the sensor region of the SRM over a distance longer than the length of the response functions. The dipole we used was the AGICO cube calibration standard for the JR-6A. This 8 cm^3 cubic standard has an intensity of 7.94 A/m and a magnetic moment of 6.35×10^{-5} Am^2. The AGICO cube standard has a thin strip of highly magnetized material set in the center of the plastic cube. The small size of the magnetized strip makes the AGICO standard a fair approximation of a point dipole, and so this sample was used to map the responses of the coils.

The dipole must be measured three times with the dipole oriented in turn along the X, Y, and Z-axes of the magnetometer. The resulting curves should look

somewhat like a normal distribution with the peak value corresponding to the moment of the calibration standard (Figure 3). As discussed above, these curves are normalized and the area under the curve is computed (we used the "Integrate – Area" function under the macros menu in KaleidaGraph, which also appropriately subtracts the areas associated with the negative side lobes). The area corresponds to the integrated response function, from which the effective length is calculated.

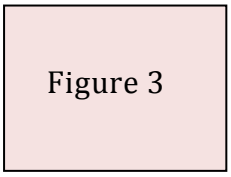

Figure 3. Normalized response functions for the new SRM, with peak moment values listed in the key.

To understand why the area gives the response function length, imagine that the moments measured for the axes were boxcar shaped with a peak value equivalent to the moment of the standard and that the boxcar extended ±2 cm from when the standard was in the center of the coils. After normalizing this boxcar, it would be easy to see that the sensor coils sense the sample over a 4 cm length and that the area under the boxcar was 4. The actual shapes of the response curves are peaked about the sensor location and the coils sense the sample less the further it is from the center of the coils. Integrating the normalized form of these real response curves yields an area equal to the effective length L_i.

The response curves were measured by placing the AGICO cube standard in the discrete sample tray in the 20 cm position and measuring every 2 mm from 0 to 40 cm along the track. For all three axes, the peak value occurred at 21.2 cm rather than 20 cm. Positioning errors of a centimeter may not be uncommon given the variable stretch in the cable. Even so, we recommend that additional positioning tests with the discrete tray be conducted and the distances to the center of the discrete sample holders adjusted appropriately in the software.

The peak values for all three axes of the SRM were all consistently lower, $\sim 6 \times 10^{-5}$ Am^2, than the expected value of 6.35×10^{-5} Am^2, which amounts to about a 5% difference. This could be due to real calibration difference between the SRM and JR-6A or due perhaps to decay in the calibration standard. We discuss further comparisons between the SRM and JR-6A magnetometers below.

The response function lengths were determined to be:

$L_x = 7.357$ cm
$L_y = 7.224$ cm
$L_z = 9.115$ cm

The response function lengths used on Expeditions 366-368 had been estimated using the width of the response curves at half their peak value.

Old L_x = 7.627 cm
Old L_y = 7.432 cm
Old L_z = 8.272 cm

The difference in the new and old values results in X and Y intensities that are about 3% larger when the new functions are used and a Z intensity that is about 9% smaller. The declination is affected negligibly by this change but the inclination will be as much as 4° shallower (depending on the remanence direction) using the new response function lengths.

The Magnetic Field Within the SRM

A 3-axis fluxgate magnetometer was used to measure the field within the sensor regions. The fluxgate was inserted inside a plastic holder that was placed in the sample tray at 145 cm. The field at this point is just the ambient field, i.e., the geomagnetic field plus the field related to the ship environment, which varies significantly with time due to ship motion and nearby personnel and electronic devices.

We were primarily concerned with the trapped field in the sensor region. The sensors are centered at 295.7 cm from the home position on the track. When the fluxgate was moved to this position, the field values, which are given relative to the magnetometers SQUID axes, were:

X-direction = -0.9 nT
Y-direction = -0.1 nT
Z-direction = -1.3 nT

These are all sufficiently small that it was deemed unnecessary to attempt to trap a lower field.

We also measured a magnetic profile along the track starting at 145 cm from the home position and continuing within the shielded area. The data were recorded with a program called DAFI, which appears to have scaled the meter readings into nT incorrectly. The relative variations, however, provide useful information and were scaled roughly to values measured directly with the fluxgate (Figure 4). The highest values ($\sim 10^5$ nT) occur outside the shielded area and are caused by the ambient field. The field values decrease by about two orders of magnitude about 25 cm inside the entrance of the first small diameter shield. Significant highs ($\sim 10^3$ nT) occur at the shield couplings at the back of this small diameter shield and the front of shield for the sensor unit (~227 cm from the home position), at the back of the sensor unit and the front of the in-line AF unit (~363 cm from the home position), and at the back of the AF unit (~439 cm from the home position).

Figure 4

Figure 4. Total magnetic field profiles within the shielded portion of the SRM system. All distances are given in centimeters from the Home Switch. The total field values recorded in program DAFI needed to be scaled to measurements made manually, and should be considered only as crude estimates until the program has been more thoroughly tested.

Attempts have been made in the past both on board and by the vendor to minimize the field at these joints, but they are still high enough to be of concern. The total field within a 30 cm wide region within the AF unit was consistently <40 nT. As discussed below in the section "AF Demagnetization Comparisons and Spurious ARMs" the new AF unit was tested at high fields to see if it would generate spurious ARMs, which were common in the old SRM. The new unit showed no evidence of spurious ARMs, which presumably indicates the fields are sufficiently low within the shielded region in the vicinity of the AF coils.

We also noticed that the electronic 'gray' box for the 2G 600 Degausser System Controller (see Figure 1) is currently placed very close to the entrance of shield at the front of the SRM. This gray box, with "High voltage" and "Danger" labels on top of it, contains many capacitors and other electronic elements. It is conceivable that the box could produce undesirable noise when the capacitors discharge and produce magnetic fields. Since magnetic field intensity decreases rapidly with distance (as $1/r^2$), it may be desirable to move the box some distance away from its current position, if that is possible. We recommend that the field be measured around the box while a sample is being demagnetized to assess if it is producing fields large enough to impart spurious magnetizations.

Radio-Frequency Interference from Cell Phones and Other Electronics

Any device that emits radio-frequency (RF) electromagnetic waves in the vicinity of the SRM is very likely to interfere significantly with the measurements. Cell phones are the primary concern when they not in "airplane mode" because they can induce large numbers of flux jumps instantaneously. The number of flux jumps is generally too large for on-going measurements to be of use. In such cases, the measurement generally needs to be aborted and then repeated when the offending devices have been removed, turned off, or put in airplane mode.

During the testing period, there were several groups of visitors touring the JR Core Deck Lab, carrying various active mobile phones and RF-controlled

camera flash units. The presence of these devices produced flux jumps that were observed to occur synchronously with their operation.

Wi-Fi communication does not seem to have any deleterious effect. Hence, cell phones can be used for their camera and other non-communication functions, but must be set to airplane mode when anywhere on the Core Deck Lab.

Improved Shielding for the AF Cables

One of the primary recommendations made during the *JR* Shakedown cruise (Expedition 320T) and the following cruise (Expedition 320) was to ensure the cables that ran into the old SRM were shielded, particularly those related to the AF unit. The new SRM has cables that are not shielded at the junction with the magnetic shield (Figure 5). This flaw provides a pathway for RF electromagnetic fields to enter the sensor region, causing flux jumps. This should be fixed and tested by using a RF transmitter (such as a cell phone) near the AF unit. Proper shielding definitely will reduce the potential for flux jumps.

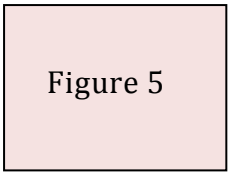

Figure 5. The cables for the AF unit that enter the magnetically shielded region have incomplete cable shielding, which allows external electromagnetic waves to interfere with the SQUID signal.

Establishing the Noise Level

To establish the noise level of the new SRM, we cleaned the tray with Windex and then AF demagnetized it at 30 mT. The tray was measured to obtain a tray or holder correction, which is referred to as the "background" correction in the IMS software. We then measured an empty tray as if it was a section half. This measurement was drift and background corrected. The resulting moments are a good approximation of the noise level of the instrument (Figures 6 and 7).

We noted that the new IMS software uses the drift correction to also account for the initial offset in the SQUID electronics from zero. This results in the raw meter measurements (referred to as X-Meter, Y-Meter, and Z-Meter) being identical to the X-Moment, Y-Moment, and Z-Moment in the data file. This should not be the case. Instead, the first raw meter value for the X, Y, and Z-axes, respectively, should be subtracted from all the X, Y, and Z Meter values to give the X, Y, and Z Moments. This initial measurement is recorded when the top of the sample tray is 326 cm from the home position, which places it 30.3 cm from the SQUID sensors. This value should always be 0.0 for the X, Y, and Z Moment values. The drift is then corrected based on the time a measurement is made,

assuming a linear interpolation between the time of the initial measurement at track position 326 cm and the final measurement, which is made when the top of the tray is at a track position of 106 cm, at which point the bottom of the tray will be 34.7 cm past the SQUID sensors for a tray that is 155 cm long. The drift corrected values in the data file in columns labeled X-Moment DC, Y-Moment DC, and Z-Moment DC are the correct values, but include both a correction for the initial meter offsets and the drift correction. The background correction is applied to the drift corrected data to give the X-Moment DBC, Y-Moment DBC, and Z-Moment DBC values, which are also computed correctly. Hence, this error does not affect the accuracy of the drift and background corrected data from previous cruises.

Once this error in the data file is corrected, the true drift correction changes the raw moments imperceptibly, which generally should be the case because drift of the instrument is small over the time range of a measurement. The drift correction can be large, and not particularly accurate, when flux jumps occur. The drift corrected data in Figure 6 illustrate that a noise level better than about 1×10^{-9} Am^2 can be attained even without background correction, with the exception of measurements made near the knot that connects the tray to the cable at the home position (track position = 0 cm), which are as large as $\sim 1 \times 10^{-8}$ Am^2 (the knot is visible in Figure 1).

In contrast, the background correction is less than 5×10^{-10} Am^2 at the knot and less than 2×10^{-10} Am^2 elsewhere (Figure 7). For a typical core section, a moment noise level of 2×10^{-10} Am^2 would equate to being able to measure split-core samples with intensities $>1.5 \times 10^{-6}$ A/m or discrete samples with intensities $>2.5 \times 10^{-5}$ A/m. This noise level is nearly identical to that which could be attained with the old SRM, e.g., see the Paleomagnetism Explanatory Notes for Leg 206 (Shipboard Scientific Party, 2003).

Dirt in the knot, which produces moments of $\sim 1 \times 10^{-8}$ Am^2, is the primary source of noise. Likewise dirt in the tray or on the core liner can be expected to be a source of noise of similar or larger size when conducting measurements on core sections during expeditions. While the noise level of the SRM is very small, the practical noise level is realistically an order of magnitude higher for core sections, which reside inside relatively dirty core liners. Thus the minimum intensities that can be measured are similar for split-core sections and discrete samples. Overall, one should expect noise levels comparable to the signal for magnetization intensities less than about 5×10^{-5} A/m (5×10^{-8} emu/cm^3).

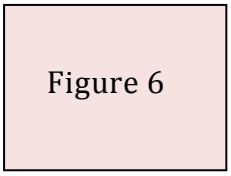

Figure 6. Magnetic moments for a clean empty sample tray after being drift corrected and after the background correction. The data before the drift correction (not shown) differ imperceptibly from the drift-corrected moments. The combination of the drift plus the background correction, which is virtually identical to the background corrected data, is shown on an enlarged scale in Figure 7. The high values near 0 cm are caused by the knot in the cable that connects the tray to the cable.

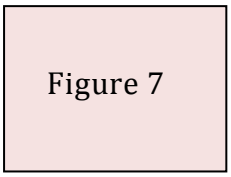

Figure 7. Magnetic moments for a clean empty sample tray after being both drift corrected and background corrected.

Split-Core Cross-Sectional Area Variations

The new magnetometer software uses a larger cross-sectional area of 17.5 cm^2 for APC split cores relative to the old SRM software value of 15.59 cm^2. This equates to using an internal core-liner radius of 3.34 cm rather than 3.15 cm. The true radius of the core material varies, but must be less than or equal to that of the core liner. Core liners are currently purchased with a specified internal diameter of 3.30-3.32 cm. Generally the core liners are filled radially for APC cores, but only partially filled for XCB and RCB cores. The new software has multiple cross-sectional area options to account for the smaller diameter of XCB and RCB cores.

In the comparisons we conducted between split-core sections that were measured on the old and new SRMs, the new SRM results naturally had consistently lower intensities until corrected for this difference.

Comparison of the New SRM to the Previous SRM

Several core sections were shipped to the Shanghai port call that had been measured on the old SRM. We elected to run experiments on two contrasting archive half sections: (i) a section of lower crustal gabbroic rocks recovered during IODP Expedition 360 to Atlantis Bank on the SW Indian Ridge (360-U1473A-65R-4A). This was previously demagnetized during shipboard experiments with a maximum peak field of 50 mT and measured at 2 cm

intervals, with several core pieces retaining ~80% of their NRM (MacLeod et al., 2017); and (ii) a section of pelagic nannofossil and radiolarian ooze that crossed the Eocene-Oligocene boundary (320-U1333C-14H-4A) and contains the Chron C13R-C13N reversal. This was previously demagnetized during IODP Expedition 320 shipboard experiments in 2009 with a maximum peak field of 20 mT, and was measured at 5 cm and then 1 cm intervals (Pälike et al., 2010). These sections were measured using the new SRM prior to magnetic cleaning and after repeating the magnetic cleaning at the highest demagnetization level to which the sections had been subjected previously.

In the case of the gabbro core section (Figure 8), following adjustment for the cross-sectional area used in the SRM software (discussed above), intensities were found to match perfectly between measurements acquired on the new and old SRM systems. Declination data were also in good agreement, with only a minor and nearly constant shift of a few degrees that can be attributed to small differences in placement of the archive half section in the tray or to relative rotation of the tray during measurement. Similar differences are seen in the carbonate core section (Figure 9), and are not unexpected given the uncertainty in placement of section-halves in the magnetometer. Rotation of the tray for the new SRM should be limited to a couple degrees by the guides on the tray bottom that fit on ridges on the track. These guides were sometimes missing in trays for the old SRM, which then resulted in greater rotation of the tray as it was pulled along the track.

Inclination data from the gabbro core section are compatible between measurements, but in some intervals there are significant differences where the previously obtained values are generally higher than the new determinations. This is readily attributed to viscous decay of a vertical-downwards drilling-induced overprint (MacLeod et al., 2017) during storage in the IODP Kochi Core Repository.

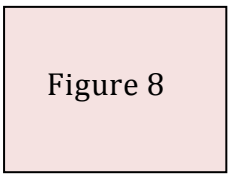

Figure 8. Variation in remanence parameters in a gabbro archive half core section measured on old and new SRM systems (following AF treatment at 50 mT).

In the pelagic ooze core section, it was necessary to apply a minor depth correction to the old SRM measurements made every 1 cm (but not to the measurements made every 5 cm). The 1 cm measurements appeared to be collected every 1.05 cm perhaps owing to a round-off error in the old SRM software subroutine that communicated with the stepper motor. The intensities for the new SRM were also adjusted such that the same core diameter was used

for the new and old measurements. Following this there is excellent agreement between the original intensities, declinations, and inclinations and those measured following retreatment at 20 mT (Figure 9). Also shown is the coeval stratigraphic interval from Hole 320-U1333B, Sections U1333B-13H-2 and -3, which had been sampled with U-channel samples and measured following 20 mT AF demagnetization using the SRM at University of California, Davis. The intensities and directions for the U-channel agree well with measurements made by the old and new shipboard SRMs. Fluctuations (spikes) are apparent in the old SRM data and the remanent inclinations for the old SRM measurements made every 1 cm do not change sign across the polarity reversal, whereas they do for the old SRM measurement made every 5 cm and for the new SRM and U-channel measurements. Both the spikes and this bias in inclination indicate that small flux jumps were occurring during the old SRM measurements, particularly for measurements made every 1 cm probably because the longer measurement duration exacerbated the effect of the cumulative flux jumps. The new SRM, in contrast, shows no signs of flux jumps.

We conclude that section half core data acquired using old and new SRM systems running under their different operating software packages are remarkably compatible, providing confidence that the new system is set up correctly and functioning properly. Moreover, the new SRM displayed better positioning control when measurements were made every 1 cm along the section and showed no signs of flux jumps, unlike the old SRM.

Figure 9

Figure 9. Variation in remanence parameters in a pelagic ooze archive half core section 320-U1333C-14H-4 measured on the old and new SRM systems. Also shown are results from U-channel samples from Sections 320-U1333B-13H-2 and -3, which are across the same stratigraphic interval as Section 320-U1333C-14H-4. The red arrow indicates the break between the two U-channel samples. The split core declinations were all rotated by 255°, which places the mean declination for the normal polarity interval at ~0°. Similarly, the declinations for the U-channel samples were rotated by 11°.

SRM Whole-Core and Split-Core Comparison

We examined new SRM data from a recently acquired, previously unsplit mudline Section 368-U1505B-1H-2. We began by measuring the NRM on the

whole-round section and, following core splitting, on both the working and archive half sections.

We were initially surprised to find the whole-round section declination close to 0°, given that the section was unoriented: this superficially resembles the radial overprint seen in archive half-sections, which would be expected to cancel for a whole-round section. We checked this by rotating the whole-round section through 90° around its long axis, and repeated the measurement. The declination rotated correspondingly, confirming that this was not a result of a radial overprint but just chance alignment of the core remanence with the arbitrarily assigned core reference frame X-axis.

Undemagnetized whole-round and archive-half SRM data show closely corresponding directional and intensity data (Figure 10). Declination data match closely for all three-section types; the agreement between the archive and working halves suggests that there is no significant radial overprint in this core section. Inclination records similarly match across all section types. Intensities are slightly offset, but vary proportionally. Differences in calculated intensity may reflect a larger cross-sectional area for the working half, which therefore contributed more moment than the archive half (The manner in which the cores are split commonly results in the working half being slightly larger than the archive half).

We conclude that there is no appreciable effect on measurement of either magnetization direction or intensity resulting from the different geometry of the whole-round and split sections, suggesting that extent and position of the sample in the core X-axis direction has no significant impact on measurement. This experiment also indicates that the IMS software correctly handles rotation of data from the SQUID coordinate system to the IODP core coordinate system for all three-section types.

Figure 10

Figure 10. Intensity, declination and intensity for whole round (red circles), archive half section (blue circles) and working half section (green circles) NRM measurements on section 368-U1505B-1H-2.

SRM Split-Core and JR-6A/SRM Discrete Sample Comparison

After the NRM of the working half of Section 368-U1505B-1H-2 had been measured, we took three discrete samples from it, in standard Japanese plastic sample holders at offsets of 10-12 cm, 57-59 cm, and 92-94 cm. The NRMs of these discrete samples were measured, and then they were demagnetized using the DTECH D2000 (2015 model) AF demagnetizer and measured at 5, 10, 15, and 20 mT steps on both the JR-6A magnetometer in automatic mode and the new SRM in discrete sample mode. The archive half section was demagnetized at the same AF steps and measured on the SRM, following routine procedures. All measurements on the SRM were corrected for drift and magnetization of the tray, and all JR-6A measurements were calibrated and corrected for holder magnetization.

Table 1 and Figure 11 compare measurements of NRM and demagnetized remanence of these discrete samples measured on the JR-6A, and measurements from corresponding positions from the archive half section demagnetized and measured within the 760R-4K SRM. The main conclusion is that the directions and intensities are quite comparable, indicating there are no gross inconsistencies between the new SRM and the JR-6A.

Even so, some small but systematic differences do occur: The JR-6A directions for the discrete samples are about 11° clockwise and 3.5° steeper than for the new SRM and the JR-6A intensities are about 5% higher than those measured on the new SRM for discrete samples and for the archive-half section. The declinations of the SRM archive-half measurements are about 6.5° clockwise of the SRM discrete samples measurements, which makes them about 20° clockwise of the JR-6A measurements. Most of the systematic declination differences could be caused by slightly rotated placement of the section half and discrete tray in the main SRM sample tray and/or by subsequent rotation of the main sample tray as it is pulled through the sensor region. This should be investigated with additional sample comparisons in which the discrete sample tray is leveled when it is placed in the main SRM sample tray and its rotation is monitored as it passes through the sensor region. The ~5% difference in the JR-6A and SRM intensities is similar to those noted during the calibration and response function measurements. In contrast, the new SRM intensities measured on discrete samples and on the archive half section differ insignificantly (<1%) on average, although individual measurements for the same demagnetization step differ by up to about 15%. Some differences between the new SRM archive half section measurements and the discrete samples presumably reflect differences in overprinting between the center of the core and its outer annulus, minor variations in remanence with position in the core, or minor deformation that occurs during collection of the discrete samples.

We conclude that overall the measurement of discrete specimen magnetization directions and intensities between the JR-6A and the new SRM are quite consistent, at least for sedimentary samples of moderate intensity. The main differences that were observed are most likely explained by poor

azimuthal orientation of the sample tray in the SRM, which produces small systematic rotation of the declination.

Figure 11

Figure 11. Comparison of discrete samples from Section U1505B-1H-2 measured on the JR-6A and the 760R-4K SRM in discrete mode, and equivalent positions on the archive half measured in the continuous section SRM mode. Each element of the figure comprises an orthogonal vector plot (left) and equal area stereographic projection (right) of remanence data (NRM and after AF treatment at steps of 5, 10, 15 and 20 mT).

Table 1. Comparison of discrete samples from Section U1505B-1H-2 measured on the JR-6A and the 760R-4K SRM in discrete mode, and equivalent positions on the archive half measured in the continuous section SRM mode.

		JR-6A			SRM discrete samples			SRM section data		
SampleID	Demag	Dec	Inc	Int (A/m)	Dec	Inc	Int (A/m)	Dec	Inc	Int (A/m)
U1505B-01H-2, 10-12 cm	0	26.6	55.9	0.264	358.5	54.9	0.246	349.15	64.77	0.299
U1505B-01H-2, 10-12 cm	5	12.9	43	0.174	358.9	36.4	0.175	345.3	40.19	0.163
U1505B-01H-2, 10-12 cm	10	14.4	34.4	0.144	358.6	35.6	0.132	344.21	30.47	0.133
U1505B-01H-2, 10-12 cm	15	12.7	35.7	0.130	356.1	36.9	0.121	343.27	29.59	0.121
U1505B-01H-2, 10-12 cm	20	8.8	37.2	0.118	359.9	38.2	0.115	341.68	30.11	0.108
U1505B-01H-2, 57-59 cm	0	3	61.4	0.265	350.2	56.2	0.255	341.97	67.02	0.292
U1505B-01H-2, 57-59 cm	5	348.9	40.7	0.166	348.5	28.9	0.190	344.46	39.38	0.151
U1505B-01H-2, 57-59 cm	10	358.7	33.7	0.134	344.1	29.8	0.121	343.19	29.42	0.124
U1505B-01H-2, 57-59 cm	15	358.9	34	0.121	342.7	29.2	0.110	342.31	28.44	0.111
U1505B-01H-2, 57-59 cm	20	346.2	30.7	0.109	342.5	29.3	0.100	341.73	28.52	0.099
U1505B-01H-2, 92-94 cm	0	346.6	66.5	0.314	349.9	61.5	0.303	342.8	67.5	0.345
U1505B-01H-2, 92-94 cm	5	12.1	49	0.194	349.4	42.8	0.198	345.47	44.04	0.171
U1505B-01H-2, 92-94 cm	10	3.7	42.5	0.154	345.8	38.8	0.138	344.92	34.5	0.136
U1505B-01H-2, 92-94 cm	15	1.6	42.4	0.138	346.8	38.7	0.123	344.01	33.45	0.121
U1505B-01H-2, 92-94 cm	20	356.3	42	0.123	344.4	39.1	0.111	343.64	32.95	0.107

AF Demagnetization Comparisons and Spurious ARMs

Experiments during some past hard rock expeditions (e.g., IODP Expedition 335; Teagle et al., 2012) had identified problems with the in-line AF demagnetization system of the old SRM at peak applied fields > 40 mT, resulting in acquisition of significant ARM components. Although weak in intensity, these components prevented identification of stable end-point directions during demagnetization. In order to test for this effect in the new SRM system, we requested three new discrete samples from core section 231R-1, recovered at Hole 1256D during IODP Expedition 312, to compare with results from corresponding points in the archive half core acquired using the old SRM during IODP Expedition 312 and extended to higher peak fields during Expedition 335 (Teagle et al., 2012).

Site 1256 restores to an equatorial paleolatitude in the Miocene (Wilson et al., 2003), and so primary remanences are expected to have shallow/sub-horizontal inclinations. Shipboard results from archive half pieces showed steep NRM directions due to an intense sub-vertical drilling-induced overprint and a migration to shallower inclinations during demagnetization up to peak applied fields of 40-55 mT (Figure 12, left hand column). Treatment at higher fields up to 80 mT then resulted in steepening of remanence inclinations and migration of points away from the origin, making isolation of characteristic magnetizations impossible. In contrast, results from demagnetization of discrete samples using the new SRM (Figure 12, right hand column) show no evidence for spurious ARM components, even at high fields up to 80 mT, allowing shallowly-inclined high coercivity characteristic components trending to the origin to be resolved clearly. These experiments demonstrate, therefore, that the new SRM represents an improvement on the old system, although we note that caution may still be required in the interpretation of data from high field treatments as ARM acquisition will be sensitive to sample-specific rock magnetic characteristics.

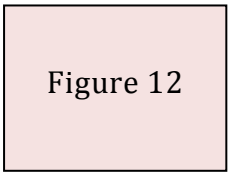

Figure 12. Comparison of shipboard archive half core demagnetization data from section 312-1256D-231R-1 (measured on the old SRM) and data from demagnetization of discrete samples performed on the new SRM during testing.

JR6 Upload

The excellent agreement between measurements performed on the new SRM and the JR-6A during testing suggests that the problems highlighted during Expedition 368 regarding correlation of JR-6A and SRM archive data do not have an instrumental origin. We therefore investigated the original data files from these experiments, and compared files produced by the AGICO Remasoft software used to operate the JR-6A with files generated by the IODP database uploader software for the instrument. Discrepancies were identified that may account for the problems reported by shipboard paleomagnetists, and the source of these discrepancies is currently being isolated and resolved by IODP technical staff. We also noted that JR-6A data files output from LIMS have columns improperly labeled as "Magnetic moment" for the x, y, and z axes that are actually intensities.

Conclusions and Recommendations

The new SRM is functioning as well as, if not better than the old SRM. It is currently capable of AF demagnetization at peak fields of 80 mT without imparting spurious ARMs, which were commonly imparted in the old SRM.

The new IMS software has an intuitive graphic user interface, which will make using the SRM and viewing the results straightforward. It allows the user to specify irregularly spaced measuring points, providing an advantage when measuring RCB cores consisting of discontinuous, variably oriented pieces. The software requires tweaking to fix some remaining bugs as discussed below. Although still under development, ancillary applications, like DAFI and Time Series Utility provide additional functionality in the lab including the collection of field profile data along the track and long-term drift, respectively. We commend IODP for these software advances.

The time available for evaluating the paleomagnetism lab was fairly limited and more remains to be done. Proposed improvements in many cases require additional measurements as well as continual observation of the shipboard instruments and environment. The following is a list of recommendations and action items that should improve the shipboard paleomagnetism laboratory and assist future lab users.

- Fix and test the uploading software for the JR-6A, and fix the column labels for JR-6A data downloaded from LIMS by replacing "Magnetic moment" with "Intensity" for the data for the x, y, and z axes.

- Add shielding to the red cables for the AF unit that connect to the magnetic shielding and make sure it is properly grounded.

- Test for flux jumps with cell phones and other devices. These tests should be conducted before and after adding shielding to the red AF cables.

During the tests, an RF transmitter (e.g., cell phones) should be used next the various magnetic shield segments.

- Add signs around the Core Lab that state "Do not use actively transmitting cell phones in this lab. Please turn your cell phone to airplane mode before entering the lab or do not bring it into the lab."

- The SRM configuration file should contain the response function lengths. This would allow corrections to be made to data files if incorrect response functions were inadvertently used during measurements.
    - The SRM data format changed significantly in the new IMS software relative to prior versions of software used with the old SRM. The prior format had been carefully vetted by the paleomagnetism community to include essential information. It would be wise to ensure that all that information is being included in the new data files and that a stable format is attained as quickly as possible.

- An error occurs in the SRM output. The X-Moment, Y-Moment, and Z-Moment columns in the SRM output files need to contain the raw moments, which are the X-Meter, Y-Meter, and Z-Meter values minus the X-Meter, Y-Meter, and Z-Meter value at the first drift measurement position.

- We recommend that calibration comparisons be conducted by shipboard paleomagnetists, who might bring along stable samples that have been accurately measured in their own labs before coming to the ship. This would allow comparison with the shipboard SRM and JR-6A and provide valuable inter-lab comparison for the paleomagnetism community.
    - These data would need to be saved on the ship over time and made available to the paleomagnetism community.

- The response function lengths should be measured multiple times to ensure their accuracy.

- Investigate how much the tray rotates as it is pulled along the track. Such rotation can bias the measured magnetic declination. If significant rotation (more than about 3°) is occurring, methods to reduce the rotation should be considered.

- Tray positioning tests should be conducted regularly. Standards or small samples should be placed along the split core tray and in the discrete sample tray at known positions. The trays should then be measured at increments of about 0.5 cm or less to ensure that the positions along the tray and at the center of the discrete sample holders are accurate to better than 1 cm. To test this for heavy split-core sections, which will

cause more stretch in the cable, the standards could be placed on top of a weakly magnetized split-core section and measured.
    - Tests conducted during the SRM assessment suggested tray position is currently off by slightly more than 1 cm. Thus, the positioning tests should be conducted as soon as possible.

- The influence of radial positioning should be investigated. The lab has a plastic holder that allows very small (mm size) dipoles to be placed at different radial distances from the axial center of the tray. We recommend thorough testing of the new SRM for sensitivity to exact radial position of discrete samples. This information can also be of use for deconvolving the data collected along core sections. The SRM team was unable to perform these tests because of time constraints and interference in measurements from cell phones of visitors during the many port call tours.

- The along-track field profile for the SRM should be measured regularly, i.e., at least every few months. The DAFI program makes this a fairly easy measurement to make. It would be particularly useful to document the magnetic field in the sensor area and in the region around the AF coils over time. Changes in the profile over time could be used to better evaluate future problems and fix them quickly.
    - DAFI should be fixed to ensure the recorded values are in nT.
    - Field profile data files should also contain metadata on the heading and latitude/longitude of the ship at the time of the experiment.

- Discard old discrete trays, particularly those that have asymmetric sample holder positions.

- Make a plaster split-core standard that can be used to train paleomagnetists who have not used a long-core SRM before.
    - This can be done by mixing plaster with a little magnetite powder or ground-up sediment that contains magnetite and pouring it into a mold. The mold need not be a single piece but could be several short pieces that fit into the Pulse Magnetizer, allowing them to be given a permanent magnetization. The pieces could then be placed in a typical section liner and left on the ship.

- Many paleomagnetists have never used a SRM, particularly one that measures long core samples. We suggest that, besides learning how to use the software and place samples in the trays, new shipboard paleomagnetists should conduct a number of measurements to improve their understanding of the SRM and boost their confidence in the data. Some basic measurements include:
    - Establish the current noise level of the SRM: Clean the tray with a cleaner, demagnetize it using an AF field of 30 to 80 mT, and

measure the tray. Then measure the empty sample tray as a fake split-core sample. Compare the results to those found in this document or in previous explanatory notes.
    - Do the same experiment as above with the discrete tray.
    - Measure a split-core sample or a plaster replica (see above)
    - Measure the JR-6A standard in the SRM. **WARNING, do not allow AF demagnetization to be used.**
    - Conduct along-track positioning tests as described above.

- Versioning information (e.g., "IMS 9.2") should be included in the name of all instrument control and measurement software used in the paleomagnetic lab, and shipboard scientists should be encouraged to record which version was used during their expedition, and any updates made during the expedition, in the Methods section of the Expedition Report.

References

MacLeod, C. J., Dick, H. J. B., Blum, P. and the Expedition 360 Scientists, 2017. Proceedings of the International Ocean Discovery Program, Expedition 360: Southwest Indian Ridge Lower Crust and Moho: College Station, TX (International Ocean Discovery Program). doi: 10.14379/iodp.360.2017.

Pälike, H., Lyle, M., Nishi, H., Raffi, I., Gamage, K., Klaus, A., and the Expedition 320/321 Scientists, 2010. Proc. IODP, 320/321: Tokyo (Integrated Ocean Drilling Program Management International, Inc.). doi:10.2204/ iodp.proc.320321.2010

Richter, C., Acton, G., Endris, C., and Radsted, M., 2007. Handbook for shipboard paleomagnetists. ODP Tech. Note, 34. doi:10.2973/odp.tn.34.2007

Shipboard Scientific Party, 2003. Explanatory notes. In Wilson, D.S., Teagle, D.A.H., Acton, G.D., et al., Proc. ODP, Init. Repts., 206: College Station, TX (Ocean Drilling Program), 1–94. doi:10.2973/odp.proc.ir.206.102.2003

Teagle, D. A. H., Ildefonse, B., Blum, P. and the IODP Expedition 335 Scientific Party, 2012. Superfast Spreading Rate Crust 4: Drilling gabbro in intact ocean crust formed at a superfast spreading rate. Proc. IODP, 335: Tokyo (Integrated Ocean Drilling Program Management International Inc.), doi:10.2204/iodp.proc.335.2012.

Wilson, D. S., Teagle, D. A. H., Acton, G. D., et al., 2003. Proc. ODP, Init. Repts., 206: College Station, TX (Ocean Drilling Program).

F1

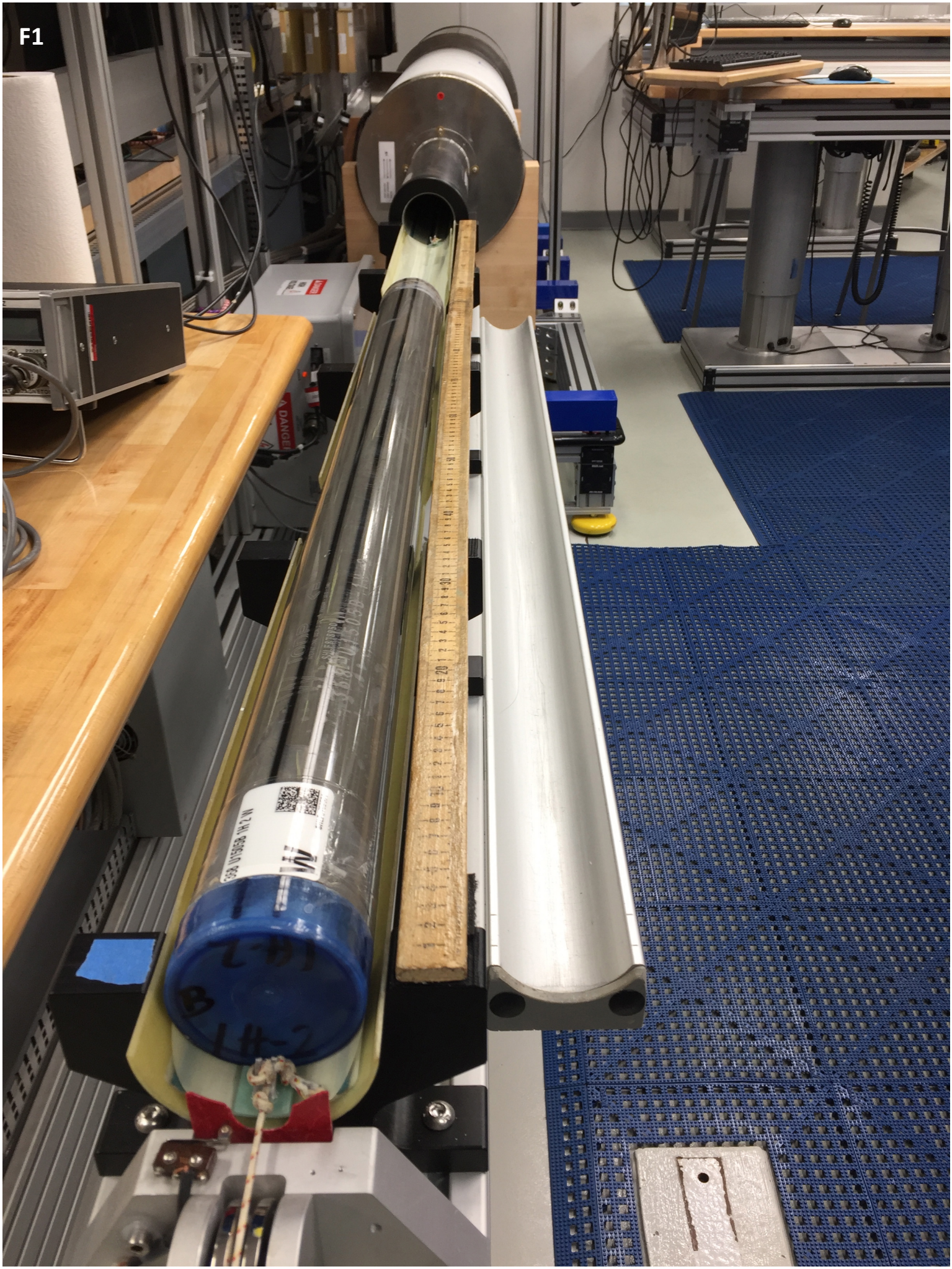

F2

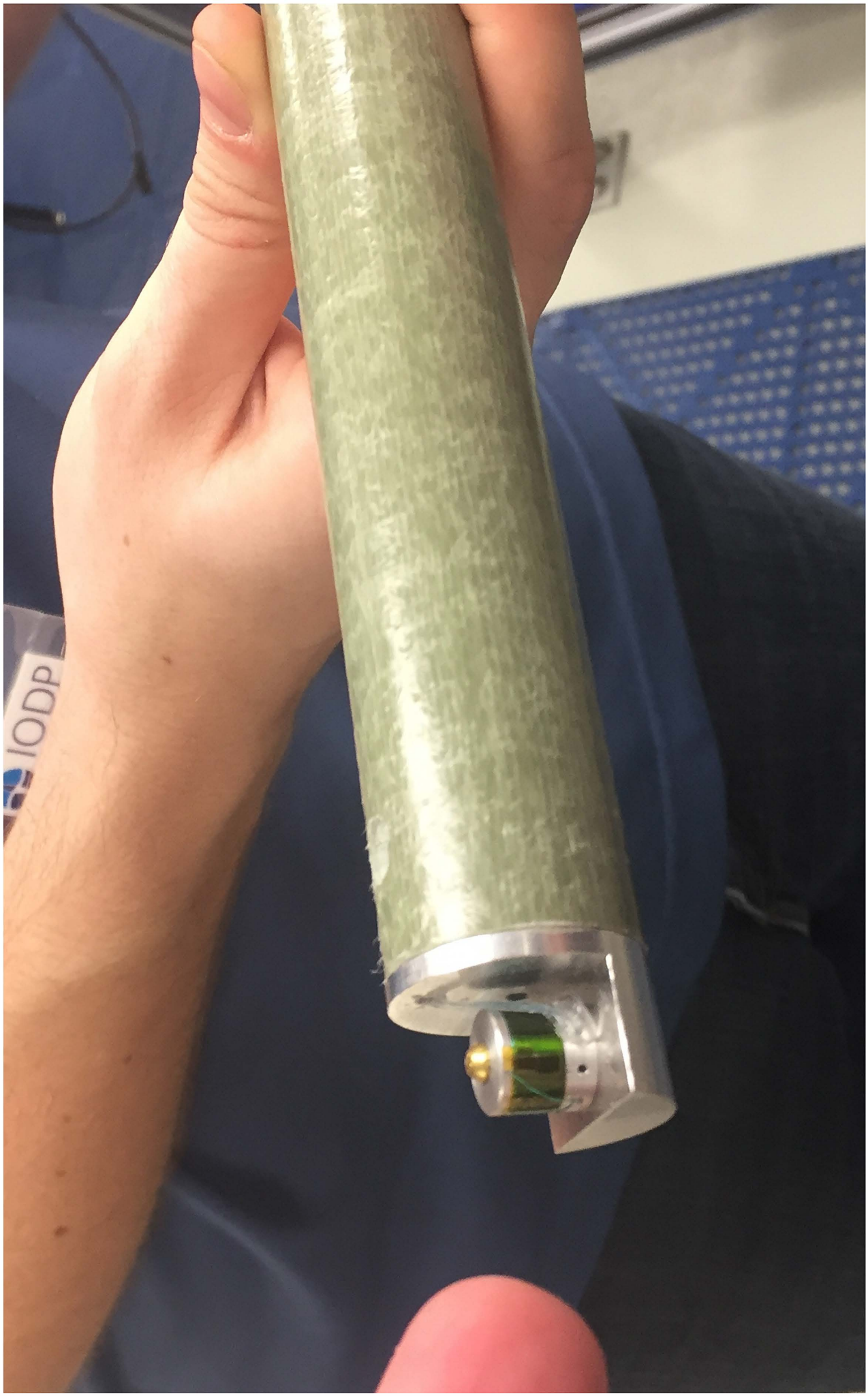

F3

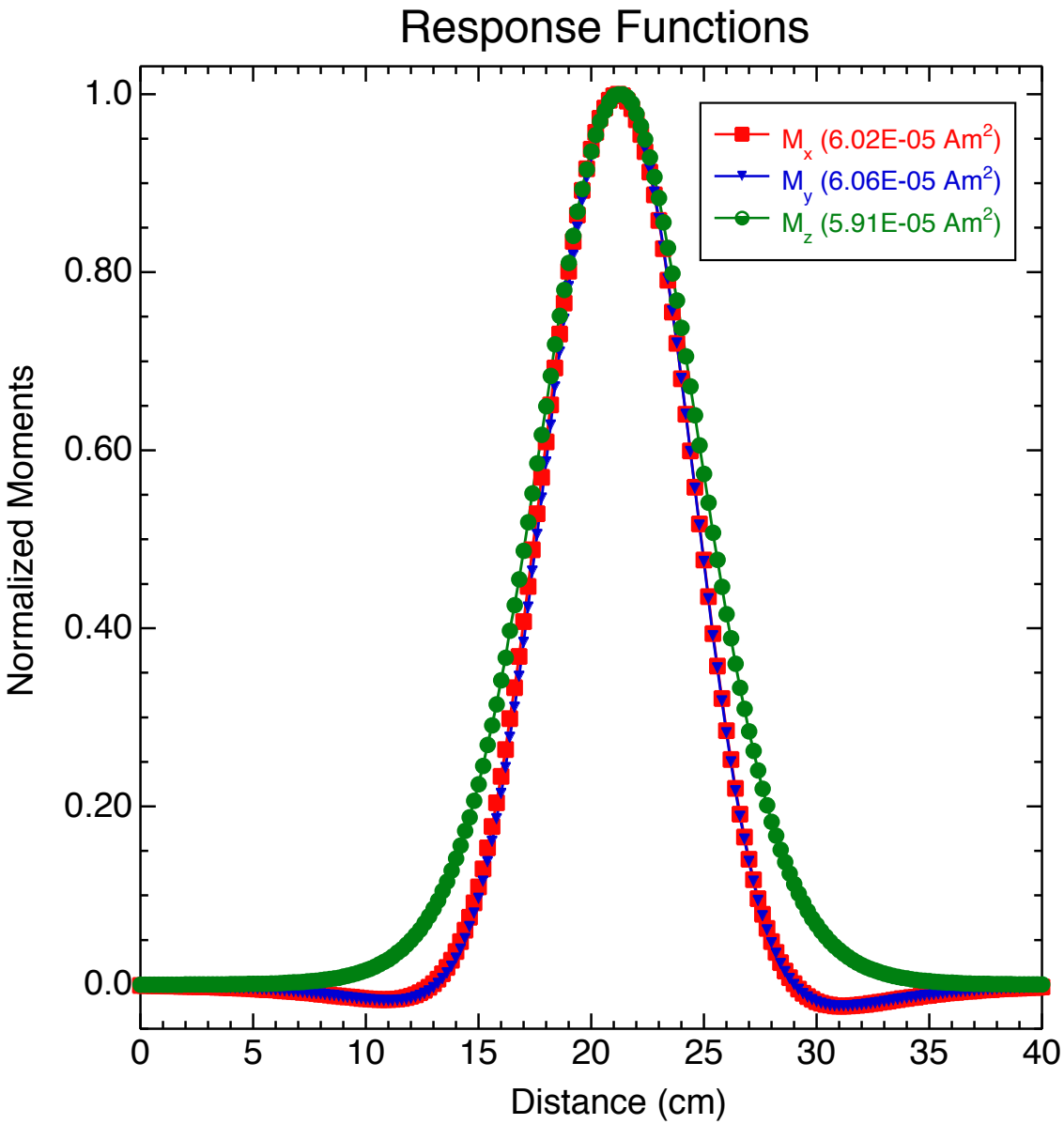
Response Functions
Normalized Moments
Distance (cm)
1.0
0.80
0.60
0.40
0.20
0.0
0
5
10
15
20
25
30
35
40
M_x (6.02E-05 Am^2)
M_y (6.06E-05 Am^2)
M_z (5.91E-05 Am^2)

F4

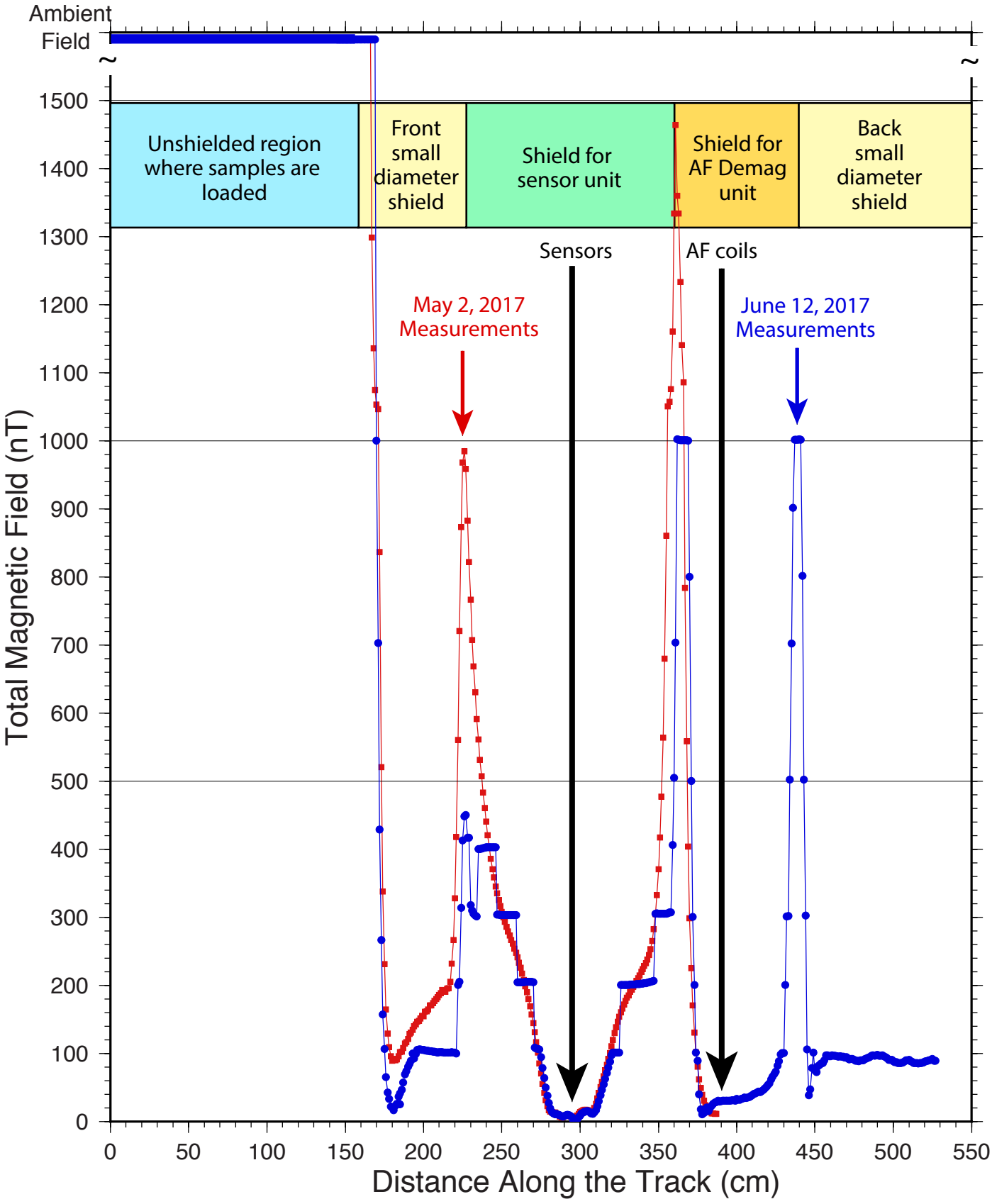
Ambient Field
Unshielded region where samples are loaded
Front small diameter shield
Shield for sensor unit
Shield for AF Demag unit
Back small diameter shield
Sensors
AF coils
May 2, 2017 Measurements
June 12, 2017 Measurements
Total Magnetic Field (nT)
Distance Along the Track (cm)
0
100
200
300
400
500
600
700
800
900
1000
1100
1200
1300
1400
1500
0
50
100
150
200
250
300
350
400
450
500
550

F5

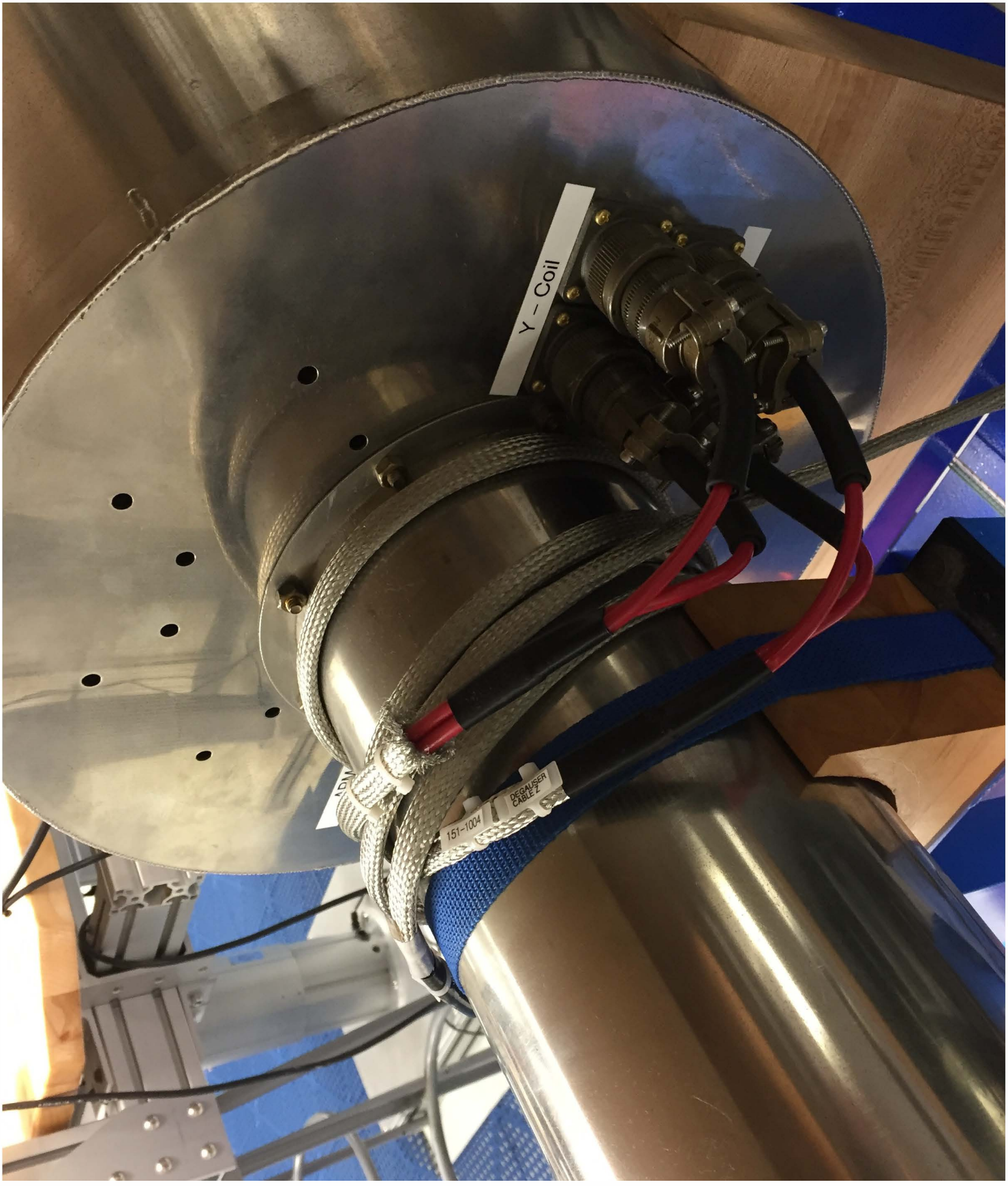

F6

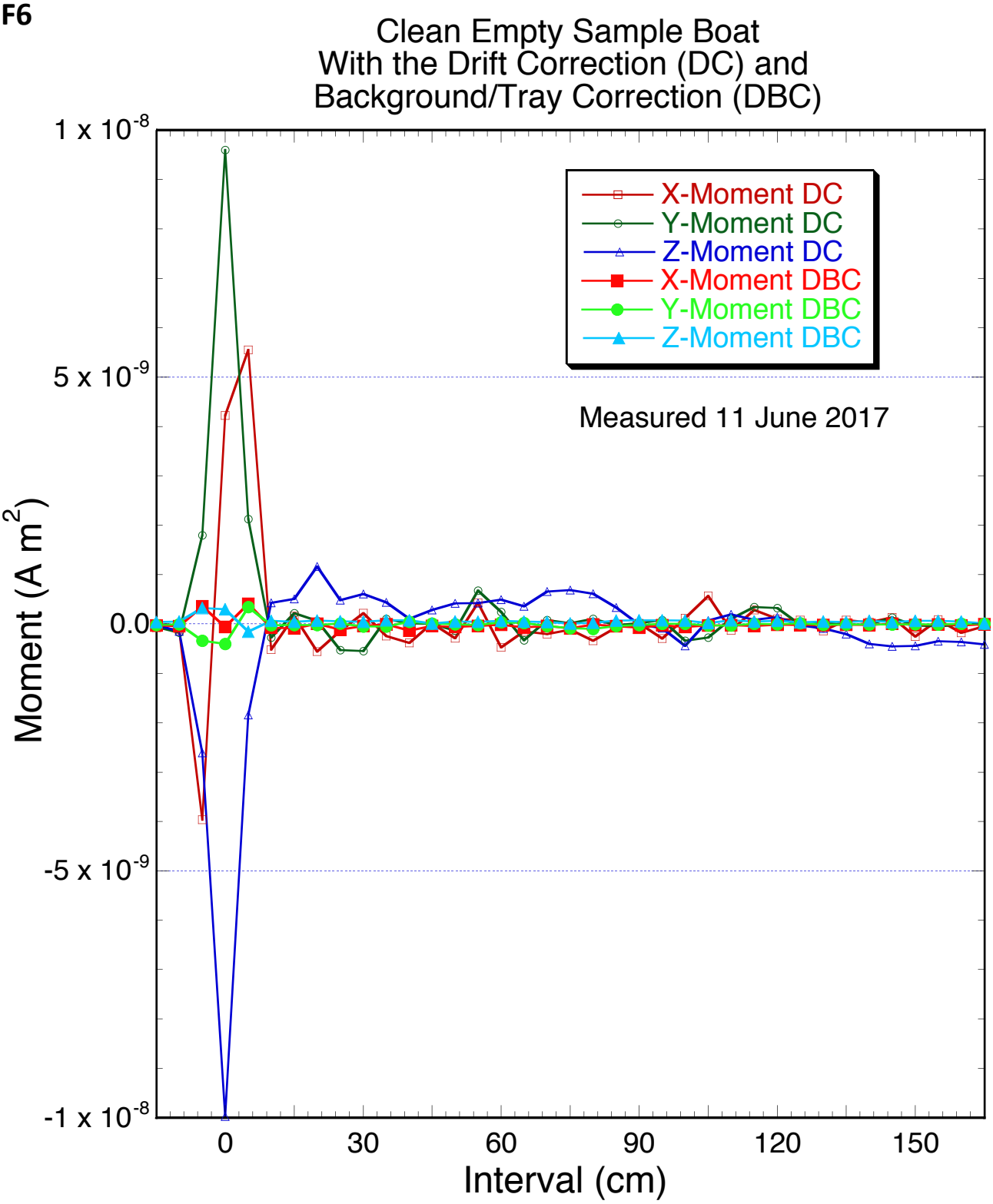
Clean Empty Sample Boat
With the Drift Correction (DC) and
Background/Tray Correction (DBC)
X-Moment DC
Y-Moment DC
Z-Moment DC
X-Moment DBC
Y-Moment DBC
Z-Moment DBC
Measured 11 June 2017
1 x 10-8
5 x 10-9
0.0
-5 x 10-9
-1 x 10-8
Moment (A m2)
0
30
60
90
120
150
Interval (cm)

F7

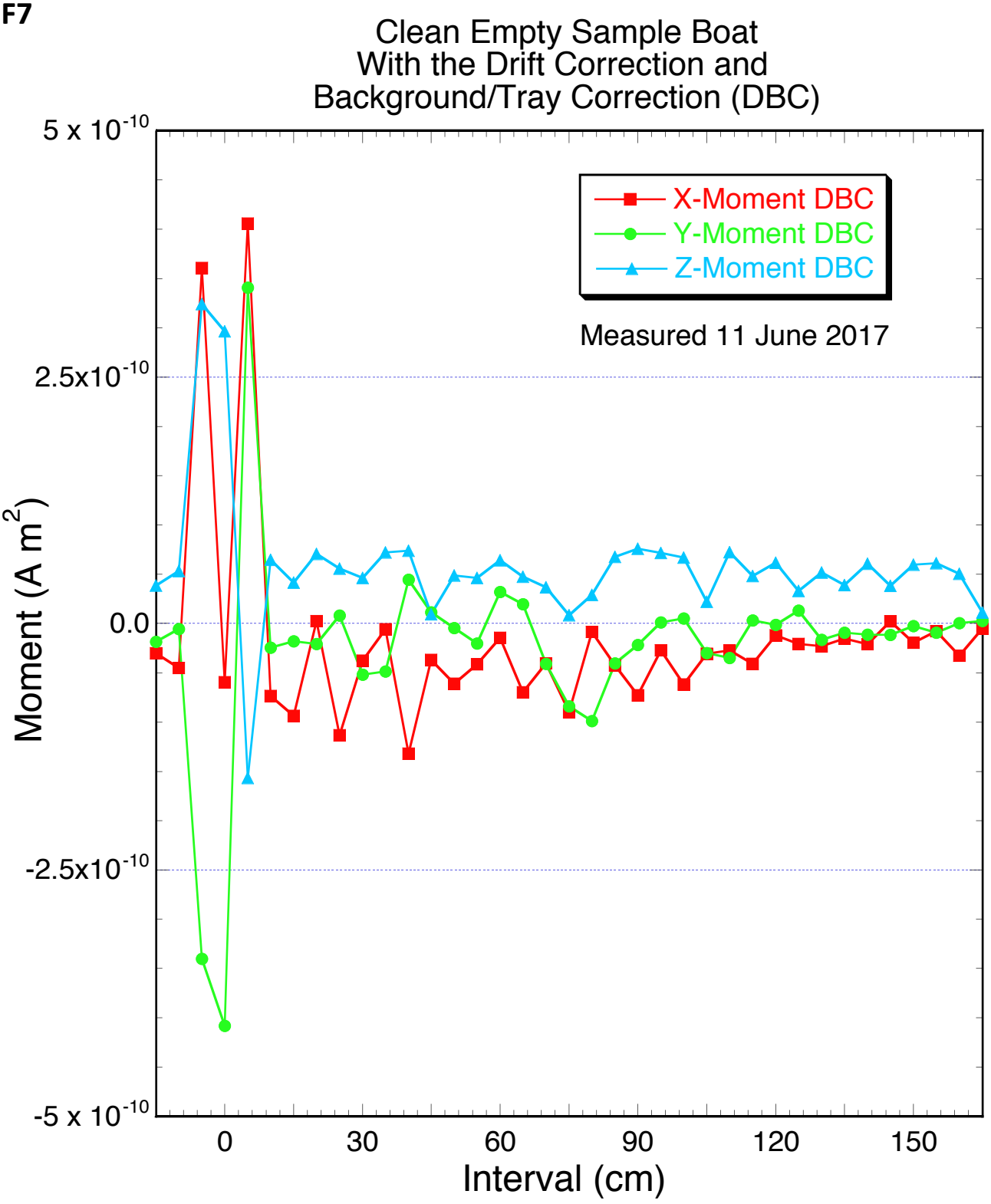
Clean Empty Sample Boat
With the Drift Correction and
Background/Tray Correction (DBC)
X-Moment DBC
Y-Moment DBC
Z-Moment DBC
Measured 11 June 2017
5 x 10-10
2.5x10-10
0.0
-2.5x10-10
-5 x 10-10
Moment (A m2)
0
30
60
90
120
150
Interval (cm)

F8

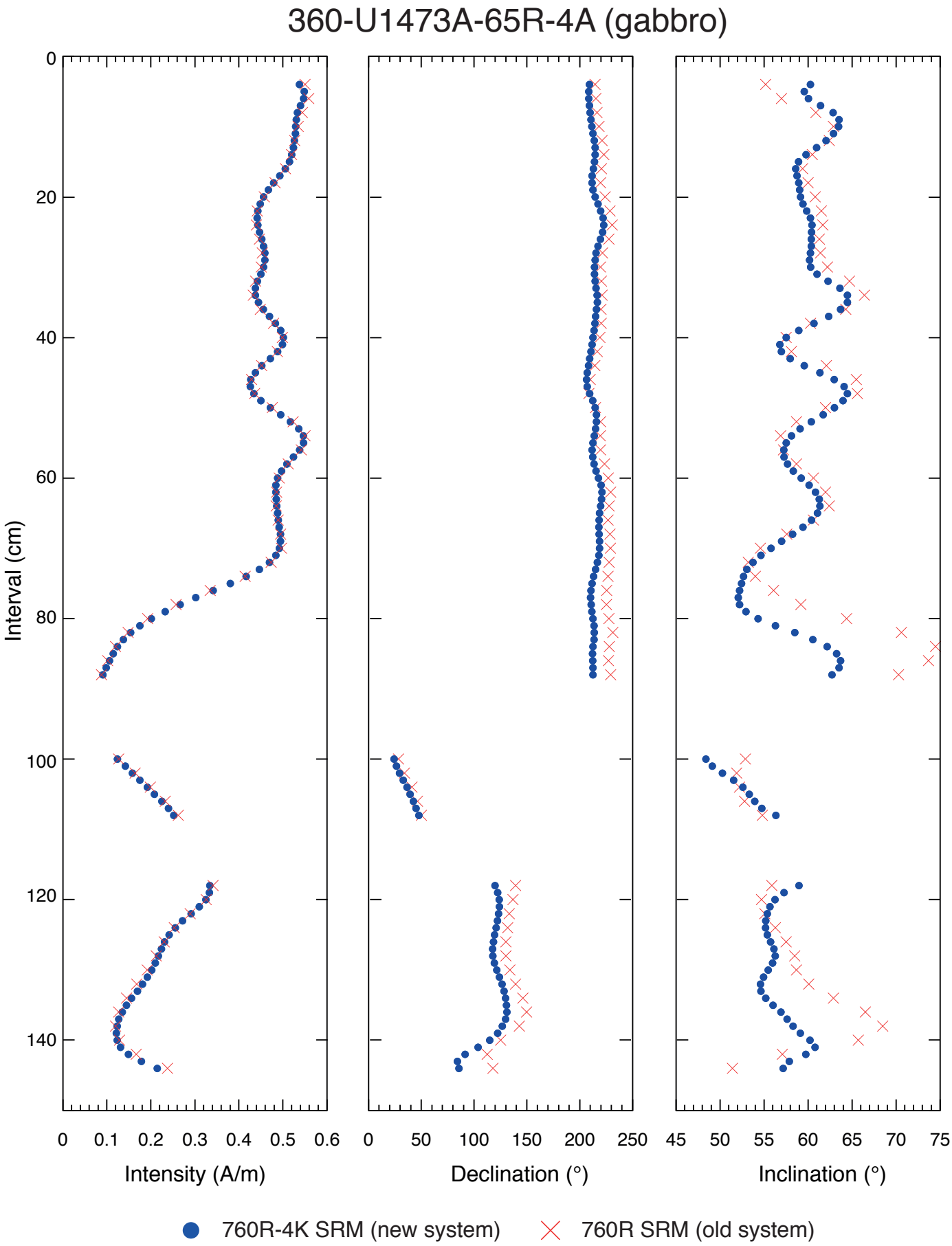
360-U1473A-65R-4A (gabbro)
Interval (cm)
0
20
40
60
80
100
120
140
0 0.1 0.2 0.3 0.4 0.5 0.6
Intensity (A/m)
0 50 100 150 200 250
Declination (°)
45 50 55 60 65 70 75
Inclination (°)
760R-4K SRM (new system)
760R SRM (old system)

F9

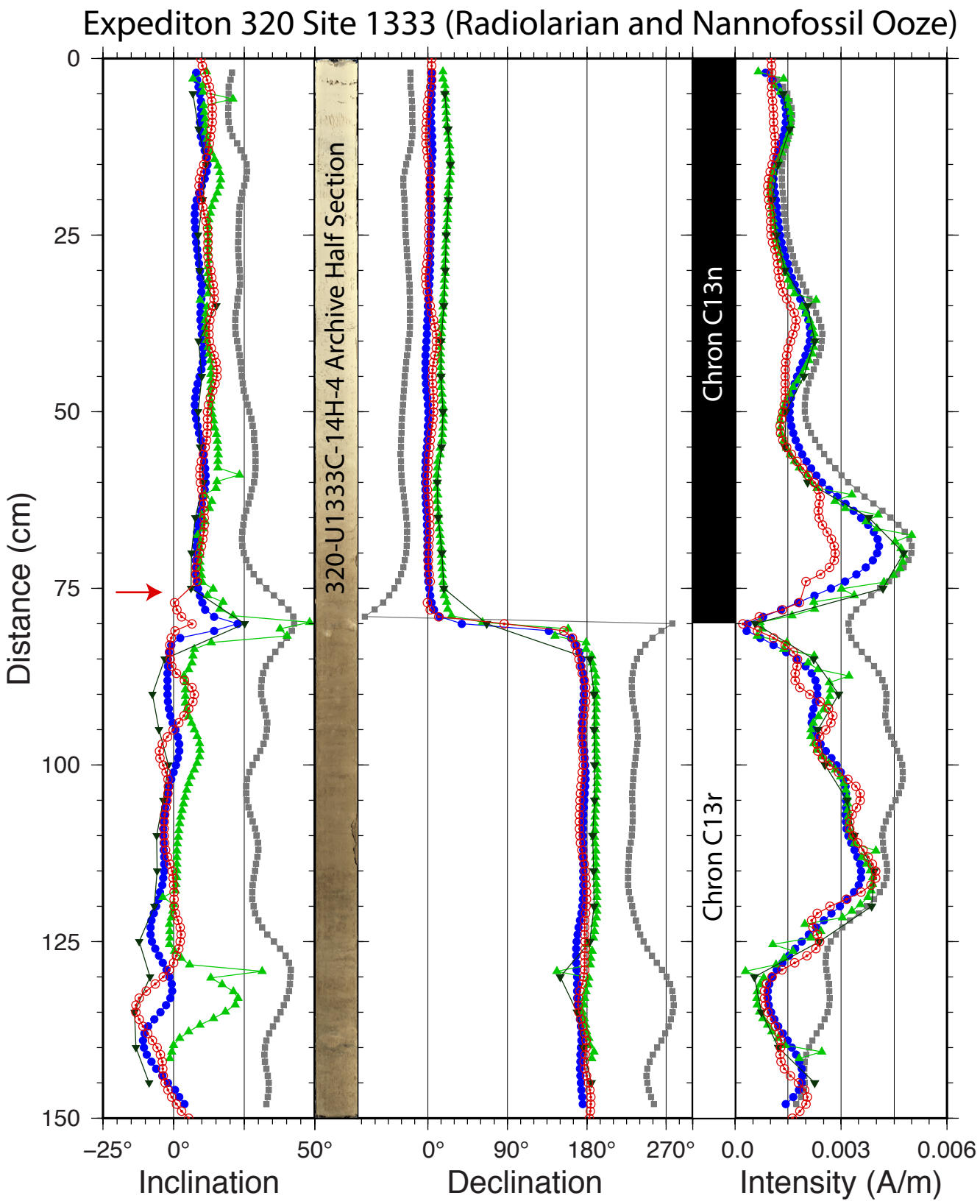

▼ Old SRM, U1333C-14H-4, Demagnetized at 20 mT on Exp 320 measured every 5 cm

▲ Old SRM, U1333C-14H-4, Demagnetized at 20 mT on Exp 320 and measured every 1 cm

■ New SRM, U1333C-14H-4, Demagnetized at 20 mT on Exp 320 but not since then.

● New SRM, U1333C-14H-4, Following 20 mT demagnetized using the new SRM in Shanghai

○ UC Davis SRM, U1333B-13H-2 and 3 U-channel samples, Following 20 mT demagnetized

F10

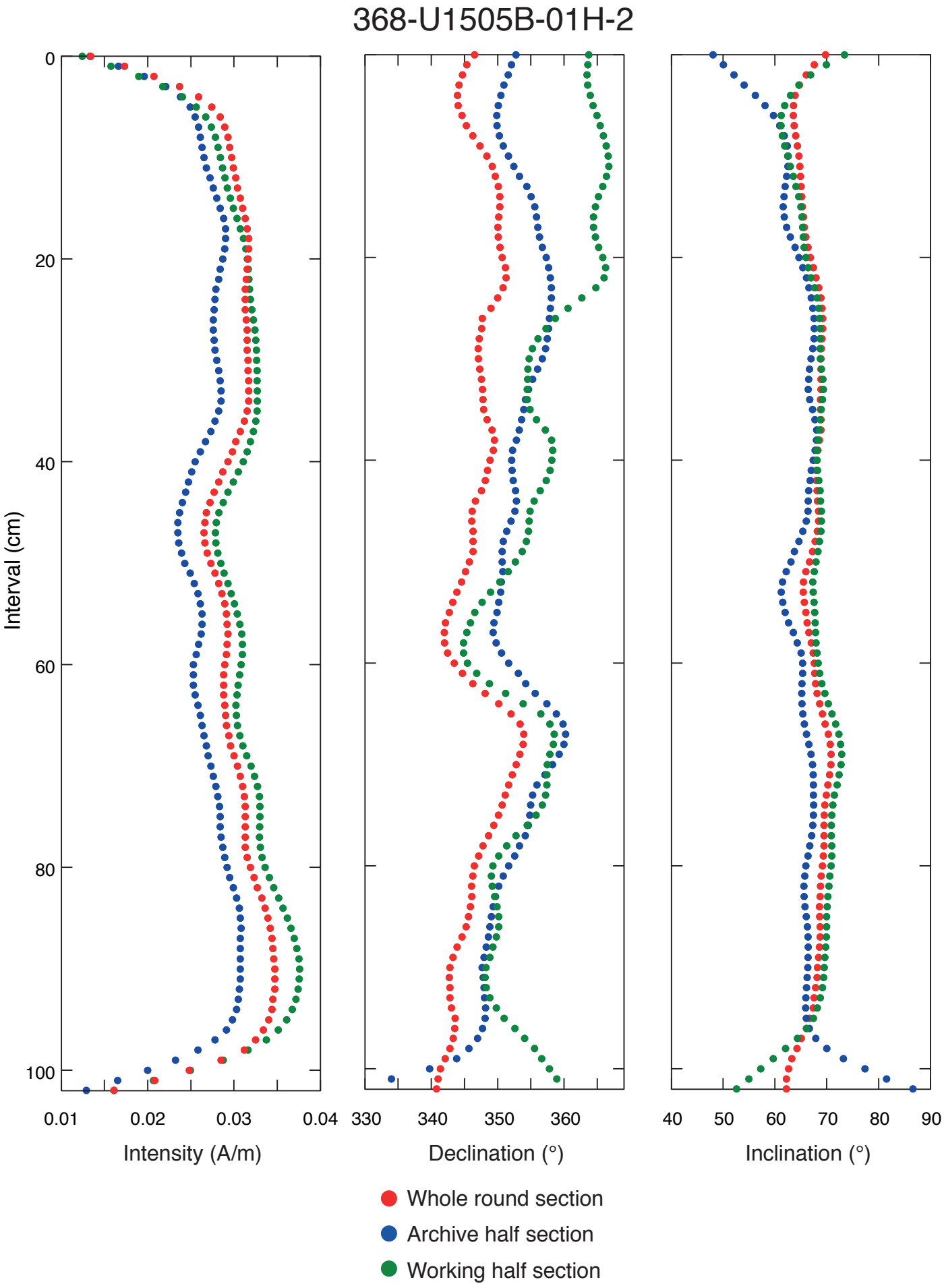
368-U1505B-01H-2
Interval (cm)
0
20
40
60
80
100
0.01
0.02
0.03
0.04
Intensity (A/m)
330
340
350
360
Declination (°)
40
50
60
70
80
90
Inclination (°)
Whole round section
Archive half section
Working half section

F11

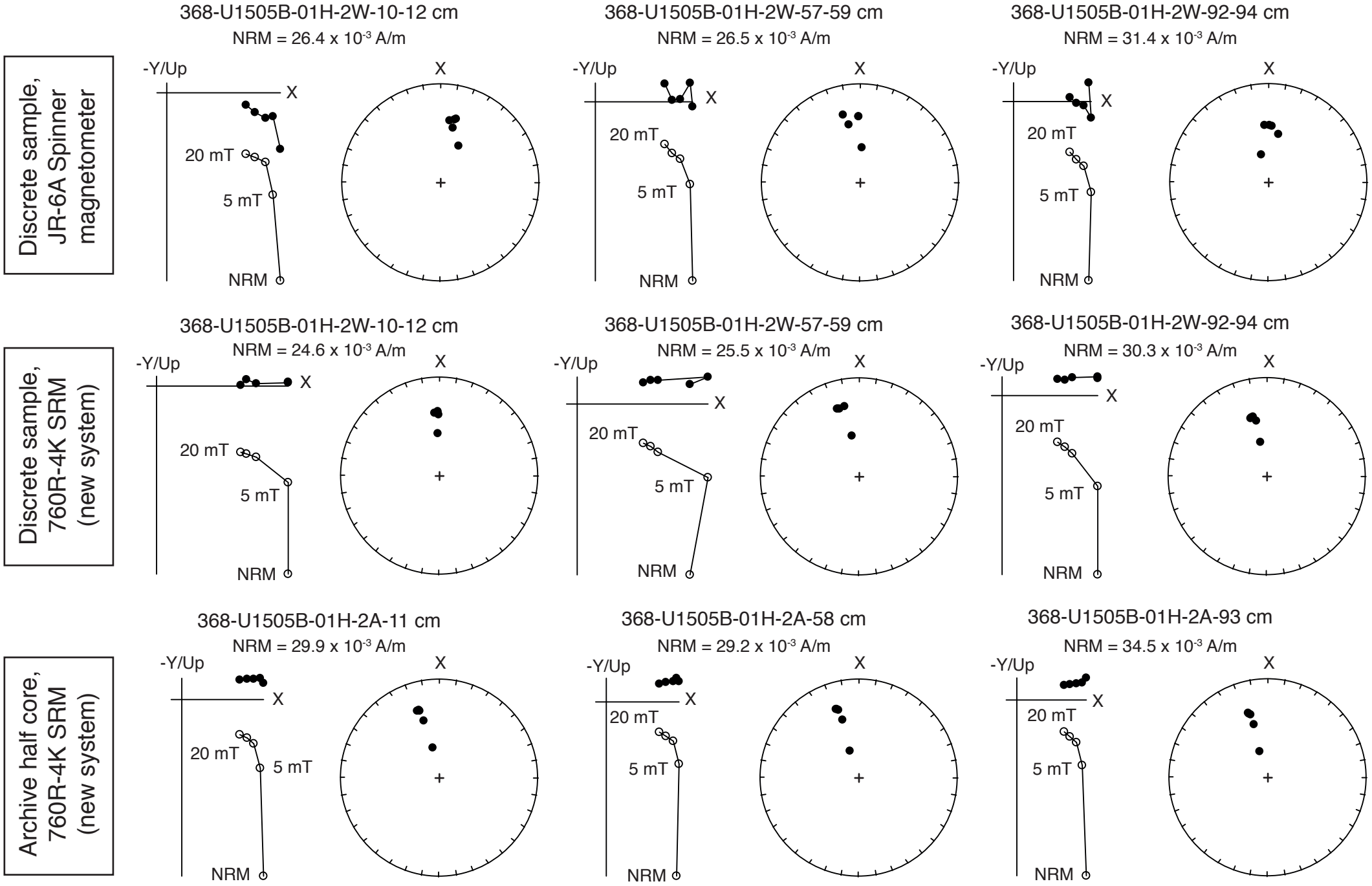
Discrete sample, JR-6A Spinner magnetometer
368-U1505B-01H-2W-10-12 cm
NRM = 26.4 x 10-3 A/m
368-U1505B-01H-2W-57-59 cm
NRM = 26.5 x 10-3 A/m
368-U1505B-01H-2W-92-94 cm
NRM = 31.4 x 10-3 A/m
Discrete sample, 760R-4K SRM (new system)
368-U1505B-01H-2W-10-12 cm
NRM = 24.6 x 10-3 A/m
368-U1505B-01H-2W-57-59 cm
NRM = 25.5 x 10-3 A/m
368-U1505B-01H-2W-92-94 cm
NRM = 30.3 x 10-3 A/m
Archive half core, 760R-4K SRM (new system)
368-U1505B-01H-2A-11 cm
NRM = 29.9 x 10-3 A/m
368-U1505B-01H-2A-58 cm
NRM = 29.2 x 10-3 A/m
368-U1505B-01H-2A-93 cm
NRM = 34.5 x 10-3 A/m
-Y/Up
X
20 mT
5 mT
NRM

F12

760R (old SRM system)

312-1256D-231R-1A-18 cm

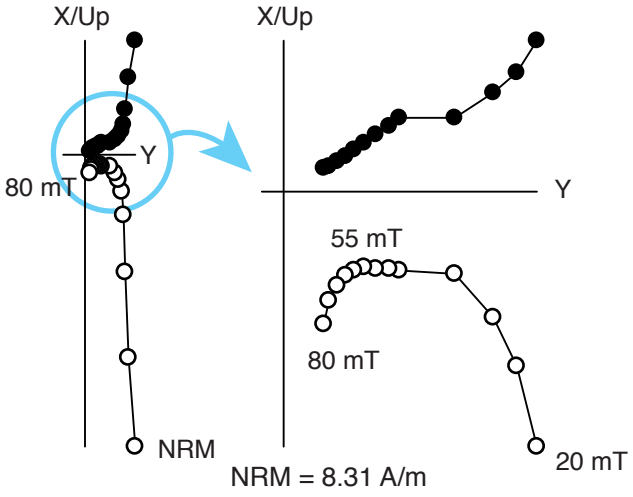

312-1256D-231R-1A-40 cm

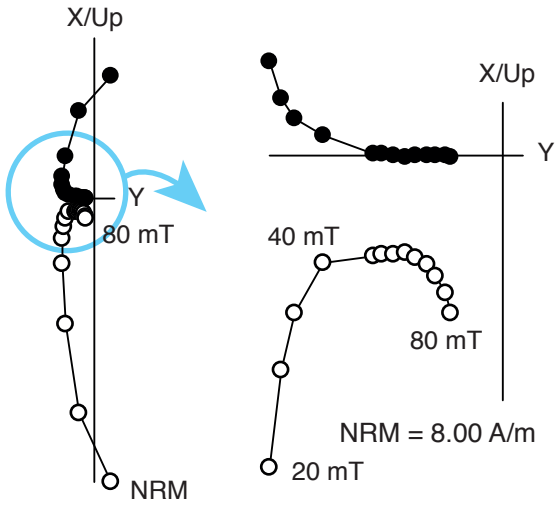

312-1256D-231R-1A-42 cm

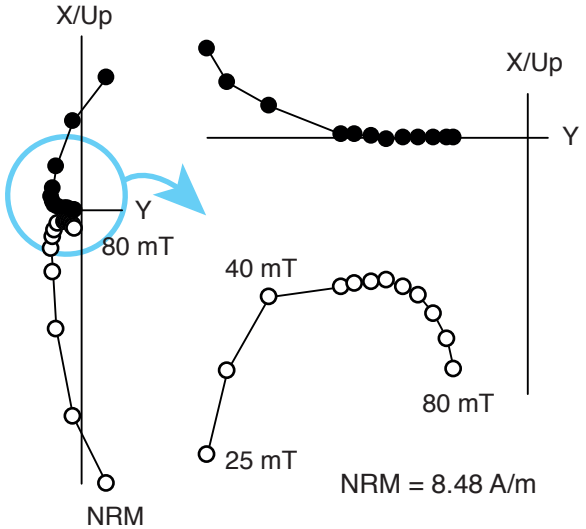

760R-4K (new SRM system)

312-1256D-231R-1W-20-22 cm

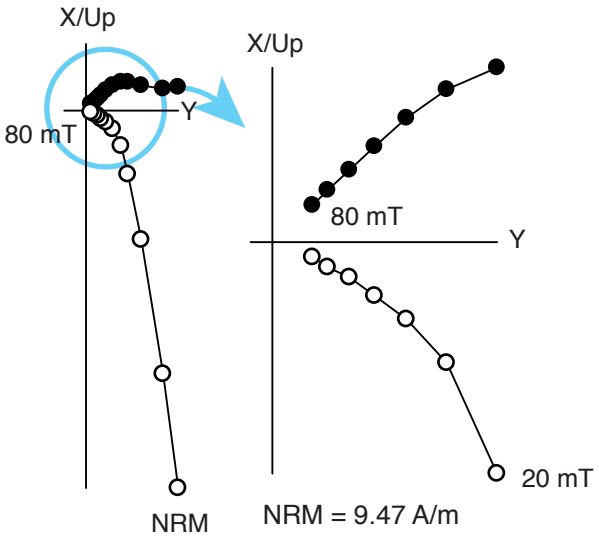

312-1256D-231R-1W-40-42 cm

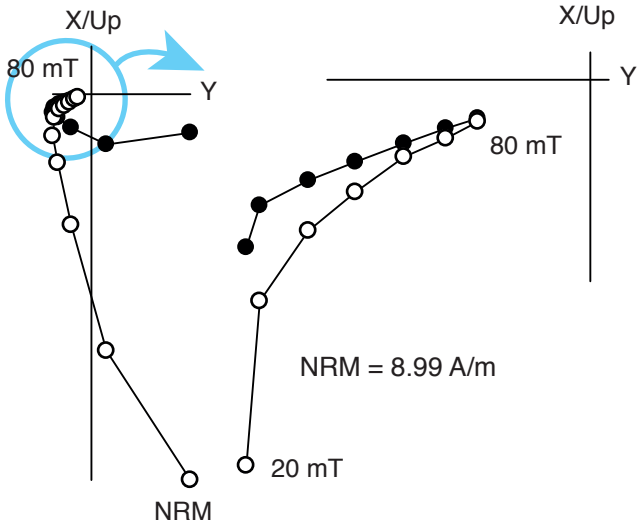

312-1256D-231R-1W-42-44 cm